

Extraction of Parameters from Remote Sensing Data for Environmental Indices for Urban Sustainability

Junichi Susaki, Supannika Pothitthep, Ryoza Ooka, Yoshihumi Yasuoka, Takahiro Endo, Yo-ichi Kawamoto
Institute Industrial Science, University of Tokyo, Tokyo, Japan
susaki@iis.u-tokyo.ac.jp

Hidenobu Nakai, Madoka Nakashima, Rei Takada
Tokyo Electric Power Company

Masahiro Setojima, Manabu Funahashi
Kokusai Kogyo Co. LTD.

Keiichi Okada
Shimizu Corporation

Abstract: Asian mega cities have continued to expand, and accordingly, various problems, e.g. social, economical and environmental problems, have been widely recognized in Asia. Especially, environmental issues caused by Asian mega cities will affect not only the areas within mega cities but also the whole area of Asian countries because the effects will be widely propagated by atmospheric or marine transportation. Authors have conducted researches related to comprehensive assessment indices for urban sustainability, named as Environmental Indices for Urban Sustainability (EIUS). In the framework of EIUS, both the environmental quality and the environmental load are focused on. An urban sustainability will be evaluated based on the scores for all categories of EIUS [1]. Most of the environmental data used in EIUS are collected from statistical data and those are restricted to point-based data. If area-based data such as vegetation distribution or urban area distribution are required, remotely sensed technique is quite useful. Remote sensing data also has an advantage to compare the parameters of different cities by the same criteria. In the present research, the applicability of remote sensing data to extract area-based environmental data for EIUS was examined. Landsat Thematic Mapper (TM) and Enhanced Thematic Mapper Plus (ETM+) images, observed in 1990s and 2000s, were used to extract vegetation index, albedo and land surface temperature. Urban areas of Bangkok in 1990s and 2000s were extracted from such parameters. Based on the acquired results, the methodology will be improved and applied to extract urban areas in other Asian mega cities.

Keywords: Environmental Indices for Urban Sustainability, EIUS, Remote Sensing Data.

1. Introduction

Environmental issues caused by Asian mega cities have been recognized to be monitored and assessed in an effective manner. While some statistics of mega cities have been reported to date, a systematic assessment is still lacking. Authors have developed comprehensive assessment indices for urban sustainability, named as Environmental Indices for Urban Sustainability (EIUS). The EIUS is based on the framework of comprehensive assessment system for building environmental efficiency (CASBEE). The CASBEE was developed for assessment of the efficiency surrounding a building. In Section 2, EIUS as well as CASBEE are described. Considering implementation of EIUS, data accessibility is quite a difficult issue. Therefore, we examined the feasibility of application of satellite remote sensing data.

2. Framework of EIUS

1) CASBEE

In the field of architecture where mass resources and energy are consumed, “sustainability” has been one of the most important keywords. Development of techniques and policies for sustainability is quite inevitable. CASBEE aims to promote proactive decisions in terms of environmental effects caused by construction and management of buildings. And, it assesses based on the items which should be pursued proactively in future. Therefore, CASBEE focuses on environmental functions of buildings, not on all of the functions of qualities of buildings [2].

A basic concept of CASBEE is shown in Fig. 1. In CASBEE, “Virtual boundary” is assumed to discriminate a space inside boundary from a space outside boundary. The space inside boundary refers to the quality of the space mainly provided by the building. This is called as “Environmental quality”. On the other hand, the flow from the inside to the

outside of boundary can be regarded as a negative load to the environment. This is called as “Environmental load”. In Fig. 1, BEE (Building Environment Efficiency) can be defined as the ratio of “Environmental quality” to “Environmental load”. Such a simple index can represent both quality and environmental load of a building [2].

Fig. 2 shows an example of assessment of environmental quality and load based on BEE. In CASBEE, there are five scores such as S, A, B+, B- and C. In the space of “Environmental load – Environmental quality”, each score has its own domain. If BEE is higher, a better score will be given. Such an assessment based on BEE value enables the comparison between different buildings. This framework of CASBEE can be applied for environmental indices for urban sustainability, or EIUS. The details on EIUS are described in the following subsection.

2) Concept of EIUS

EIUS was created as an index to enable the assessment and comparison of urban sustainability. EIUS is based on the concept of CASBEE. Tab. 1 shows EIUS framework. In the EIUS, there are two types of categories such as “Quality life of inside city” and “Environmental load”. Each category has hierarchical structure consisted of the first classification and the second classification items. In the category “Quality life of inside city”, there are three first classification items; “Environment / Public Health”, “Public Function / Public Services” and “Safety / Security”. On the other hand, the category “Environmental load” has three first classification items such as “Energy”, “Resources” and “Environment over wide area”.

Tab. 1 also represents the examination results of data availability in Bangkok. Authors have contacted ministries and departments of Thailand, and examined data availability. The “Source” in Tab. 1 means ministries and departments of Thailand which can provide the data. Regarding the data accessibility, most of the data were obtained a few to several weeks after official documents were sent to them. Gray column shows the data were not available. In the case of Bangkok, it was found that most of data required in the current framework are available.

3) Difficulties in Data Collection for EIUS

Even though data collection was successfully conducted in Bangkok, it is not expected to obtain as much data as in other mega cities. Therefore, the data items should be flexibly changed in accordance with the real data accessibility. Simultaneously, we have to consider the data source independent of statistical data collected by organization in different countries. Another reason for the necessity of another data source is to apply the same criteria for data collection. While the statistics are useful for the national analysis, non-unified criteria for the statistics will cause confusion for the international analysis. Our final goal is to assess and compare the environmental sustainability in many mega cities. Therefore, we have to compare the statistics collected in different countries.

Remote sensing has a strong advantage for such problems. The remote sensing, especially satellite remote sensing, can observe land, ocean and atmosphere from the space. In most of applications, remote sensing data are converted into physical parameters or indices. The quantitative and qualitative analysis based on the same criteria can be implemented by using remote sensing data. Moreover, most of remote sensing data are processed as images, and then area-based information can be derived. Area-based information is quite effective to grasp urbanization.

Another advantage of remote sensing data is periodical observation. We have different types of earth observation satellite and sensors. High resolution data such as Landsat Thematic Mapper (TM), Enhanced Thematic Mapper Plus (ETM+), or Advanced Spaceborne Thermal Emission and Reflection Radiometer (ASTER) has 16-day periods. This means every 16-day, at least one image is periodically obtained. Optical sensor data are easily contaminated by atmospheric effects, e.g. clouds or aerosols. Therefore, we cannot expect too many images with good quality through a year. However, such periodical observation enables the analysis of temporal environmental change.

3. Feasibility of Data Collection by Remote Sensing

First of all, it should be clarified while EIUS mainly deals with various statistics, remote sensing has a potential to be one of the most effective data sources for EIUS. In the framework of EIUS, authors examined the feasibility of data collection by remote sensing.

In principle, remote sensing can detect the electromagnetic wave radiated or reflected from atmosphere, land or ocean. In terms of spatial resolution, recently very high resolution data such as IKONOS (1m) or QUICKBIRD (0.6m) data are available, and those data can provide the detailed spatial data. However, because of the expensive data cost, we focus on the usage of high resolution data such as TM, ETM+ and ASTER. Those costs are relatively cheap. Moreover, many Landsat TM/ETM+ images are available free of charge through the Internet [3]. Those images are geometrically

corrected, and two images observed in 1990s and 2000s are available in most of scenes. Such services are quite useful for the analysis conducted in the present research, i.e. quantitative analysis of temporal change of urban area.

As a result, Landsat TM/ETM+ images were used for the analysis in the present research. Especially, those images were used for the extraction of urban areas. Two images observed at different times enabled the comparison of the change of urban areas. As parameters describing such urbanization, three parameters were selected, i.e. Normalized Difference Vegetation Index (NDVI), albedo and land surface temperature (LST). In the following subsection, methods to derive parameters are described.

1) NDVI

NDVI has been widely recognized as useful for the studies of the land biosphere characteristics and dynamics at regional to global scales. NDVI has more sensitivity to chlorophyll and less contamination by atmospheric water vapor. NDVI is obtained through calculation of reflectances of the red and near infrared (NIR), expressed as Eq. (1).

$$NDVI = \frac{\rho_{NIR} - \rho_{RED}}{\rho_{NIR} + \rho_{RED}} \quad (1)$$

where ρ_{RED} and ρ_{NIR} denote reflectances at red band and NIR band, respectively. For Landsat TM/ETM+, band 3 and 4 are used.

2) Albedo

Land surface albedo is a physical parameter that describes the optical reflectance of the land surface. Albedo is commonly defined as the reflectance of a surface integrated with respect to both wavelength (usually between 0.3 μm and 3.0 μm) and angle (i.e. for all directions within the hemisphere above the surface) [4]. Land surface broadband albedo is the fraction of incident (shortwave) solar radiation reflected in all directions by the land surface [5]. Examples of the albedo applications include global and regional climatic models for computing the surface energy balance [6], and ecological models [7].

Liang developed conversion formulae from narrowband to broadband albedos for a series of sensors, including ASTER, AVHRR, ETM+/TM, GOES, MODIS, MISR, POLDER, and VEGETATION. The conversion formulae are based on extensive radiative transfer simulations. These formulae are used to calculate the total shortwave albedo and the total-, direct-, diffuse-visible, and near-infrared broadband albedos under various atmospheric and surface conditions [8]. The validation results for three broadband albedos (total-shortwave, total-visible and total-near-infrared albedos) using ground measurement of several cover types are presented in the paper. These results show that the conversion formulae are very accurate and that the average residual standard errors of the resulting broadband albedos for most sensors are approximately 0.02, which meets the required accuracy for land surface modeling [9].

In the present research, Liang conversion model was used to estimate albedo. Three types of albedos, i.e. total-shortwave, total-visible and total-near-infrared albedos, are available. As a result, total-shortwave albedo was selected for the analysis. Hereafter it is mentioned as “shortwave albedo” or simply “albedo”. The procedure to estimate albedo from DN value is described in the below [10].

Firstly, DN value was converted into radiance L by applying Eq. (2).

$$L_{\lambda} = (L_{max,\lambda} - L_{min,\lambda})/255 * DN + L_{min,\lambda} \quad (2)$$

where $L_{min,\lambda}$ and $L_{max,\lambda}$ are the spectral radiances for band λ at digital numbers 0 and 255. Tab. 2 shows L_{min} and L_{max} for all bands of Landsat TM and ETM+.

In the present research, Liang conversion model was used to estimate albedo. Three types of albedos, i.e. total-shortwave, total-visible and total-near-infrared albedos, are available. As a result, total-shortwave albedo was selected for the analysis. Hereafter it is mentioned as “shortwave albedo” or simply “albedo”. The procedure to estimate albedo from DN value is described in the below [10].

Then, radiance was converted into reflectance by applying Eq. (3).

$$\rho_{\lambda} = \frac{\pi \cdot L_{\lambda} \cdot d^2}{E_{\lambda} \cdot \cos \theta} \quad (3)$$

where

- ρ_λ unitless planetary reflectance;
- L_λ spectral radiance at the sensor's aperture;
- d earth-sun distance in astronomical units;
- E_λ mean solar exoatmospheric irradiances;
- θ solar zenith angle in degrees.

Tab. 3 shows Landsat TM and ETM+solar exoatmospheric spectral irradiances.

Finally, broadband albedo was estimated by applying Liang model for Landsat ETM+, expressed as Eq. (4) [8].

$$\begin{aligned}\alpha_{VIS} &= 0.443\rho_1 + 0.317\rho_2 + 0.240\rho_3 \\ \alpha_{NIR} &= 0.693\rho_4 + 0.212\rho_5 + 0.116\rho_7 - 0.003 \\ \alpha_{SW} &= 0.356\rho_1 + 0.130\rho_3 + 0.373\rho_4 + 0.085\rho_5 + 0.072\rho_7 - 0.0018\end{aligned}\quad (4)$$

where α_{VIS} , α_{NIR} and α_{SW} denote total visible albedo (0.4 – 0.7 μm), total near-infrared albedo (0.7 – 2.5 μm) and shortwave albedo (0.25 – 2.5 μm) for ETM+, respectively. ρ_n denotes reflectance of band n . In Liang, 2000, there is no model for Landsat TM. Therefore, Eq. (4) was also applied for the estimation of albedo of Landsat TM.

3) LST

Thermal band data (band 6) from Landsat TM/ETM+ can also be converted from spectral radiance to effective at-satellite temperature [10]. The conversion formula is described as Eq. (5).

$$T = \frac{K_2}{\ln\left(\frac{K_1}{L_\lambda} + 1\right)} \quad (5)$$

where

- T effective at-satellite temperature in Kelvin;
- K_1 calibration constant 1 in $W/(m^2 \cdot sr \cdot \mu m)$;
- K_2 calibration constant 2 in kelvin;
- L_λ spectral radiance at the sensor's aperture.

Tab. 4 shows calibration constants K_1 and K_2 for Landsat TM and ETM+. The effective at-satellite temperature values T are referenced to a black body. Therefore, corrections for spectral emissivity ε are necessary. Eq. (6) represents the emissivity correction to derive land surface temperature S_t .

$$S_t = \frac{T}{1 + (\lambda \times T / \rho) \ln \varepsilon} \quad (6)$$

where λ is wavelength of emitted radiance ($\lambda = 11.5 \mu\text{m}$), $\rho = h \times c / \sigma$ ($1.438 \times 10^{-2} \text{ m K}$), $\sigma =$ Boltzman constant ($1.38 \times 10^{-23} \text{ J/K}$), $h =$ Planck's constant ($6.626 \times 10^{-34} \text{ J s}$), and $c =$ velocity of light ($2.998 \times 10^8 \text{ m/s}$) [11].

Emissivity ε can be estimated in many ways. In the present research, a methodology reported in [12] is selected. Emissivity ε is expressed as Eq. (7).

$$\varepsilon = f_v \varepsilon_v + (1 - f_v) \varepsilon_s \quad (7)$$

where ε_v and ε_s denote emissivity of vegetation and soil, respectively. f_v denotes fractional cover of vegetation (0 – 1). ε_v and ε_s were assumed as 0.985 and 0.978 [13]. Fractional cover f_v can be expressed as Eq. (8) [14]

$$f_v = 1 - \left(\frac{NDVI_{\max} - NDVI}{NDVI_{\max} - NDVI_{\min}} \right)^a \quad (8)$$

where $NDVI_{\max}$ is the NDVI for complete vegetation cover, and $NDVI_{\min}$ is the NDVI for bare soil. In the present paper, $NDVI_{\max}$ and $NDVI_{\min}$ were assigned as 0.94 and 0.0, respectively. The coefficient a is a function of leaf orientation distribution with the canopy. In the present research, a was assumed as 0.6 for the application.

4) Extraction of Urban Areas

In most of applications of remote sensing data, parameters extracted from remote sensing data or original DN data are used for the classification to produce thematic map. Our purpose is to extract urban areas from remote sensing images. In usual classification, statistical classifiers have been applied. Such classifiers have severe shortcoming that they classify on pixel-basis, which tend to produce patch-like classification results. Therefore, classifiers based on image processing techniques have been examined. Recently, a software eCognition has been popular as an effective classification tool [15]. It classifies based on segmentation technique, and eCognition was used to extract urban areas in this research.

5) Case Study: Bangkok

In the present research, Bangkok was selected as a case study because we completed data collection of Bangkok regarding EIUS. The purpose is to examine the possibility to extract effective parameters related to environmental assessment in EIUS. As an effective parameter, urban area was selected. Both Landsat TM images in 1990s and ETM+ images in 2000s were obtained from Web site [3]. Two images of path 129, row 50 and path 129, row 51 were merged as a mosaic image. The observed dates are listed in Tab. 5.

Fig. 3 shows a flow of extraction of urban areas from Landsat TM/ETM images. From original DN values of band 1 to 5 and band 7, NDVI and albedos were estimated. And, LST was estimated from a thermal band data, i.e. band 6 data. These sets of parameters were calculated for TM images in 1990s and ETM+ images in 2000s. Firstly, urban areas in 1990s were extracted. eCognition was used for the segmentation and classification of urban areas. After urban areas in 1990s were estimated, the areas were used as a mask layer for ETM+ images. And then, urban areas since 2000s were extracted. Fig. 4 represents the results of urban areas extracted from Landsat TM/ETM+.

4. Discussions

Fig. 4 represents remote sensing can produce area-based information about urbanization. However, the methodology described in Fig. 3 and the results shown in Fig. 4 are preliminary. The results obtained in the present research should be examined from various viewpoints, and some improvements are required. Authors examined combinations of several parameters, i.e. NDVI, albedo (VIS, NIR and SW) and LST. Among those combinations, the combination of VIS albedo and LST was found to be effective for the extraction of urban areas. However, these combinations should be examined more.

The methodology to mask urban areas in 1990s needs discussions. In the beginning, authors extracted urban areas in 1990s from parameters in 1990s and urban areas in 2000s from parameters in 2000s, separately. However, the urban areas in 2000s were smaller than the urban areas in 1990s. The shrink of the extracted urban areas may be caused by different atmospheric conditions and different observation seasons. It is quite difficult that a perfect atmospheric correction is implemented because of lack of sufficient data related to atmospheric. On the other hand, authors assumed that the urban areas in 1990s will be urban areas even in 2000s. The methodology to use the masking is based on such an assumption. However, such assumption should be examined by referring to the existing thematic map. Validation of extracted urban areas and application of the methodology for other Asian mega cities will be examined in future.

5. Conclusions

In the present paper, authors report the framework of EIUS and feasibility of application of remote sensing data for EIUS. EIUS has a potential to enable the comparison of sustainability of Asian mega cities. However, implementation of

EIUS may have difficulty to collect data, mainly statistics. Even though statistics are collected from mega cities, non-unified criteria make the comparison between mega cities difficult. Therefore, a feasibility to apply remote sensing data was examined. Remote sensing enables the acquisition of area-based data, which is effective for understanding urbanization, and the comparison between many mega cities under the same criteria. In the present research, NDVI, albedo and LST were derived from Landsat TM/ ETM+ images obtained in 1990s and 2000s. Finally, urban areas in 1990s and 2000s were extracted, and it was found that remote sensing has a potential to be used for EIUS. The methodology utilized in the framework of EIUS should be examined.

References

- [1] Ooka, R., Yasuoka, Y., Susaki, J., Endo, T., Kawamoto, Y., Nakai, H., Nakashima, M., Takada, R., Setojima, M., Funahashi, M. and Okada, K., 2005. Development of new environmental indices for urban sustainability, *Proceeding of the Fourth International Symposium on New Technologies for Urban Safety of Mega Cities in Asia*
- [2] CASBEE Manual 1, 2003. *Institute for Building Environment and Energy Conservation (IBEC)* (in Japanese)
- [3] Global Land Cover Facility. Earth Science Data Interface, available at <http://glcfapp.umiacs.umd.edu:8080/esdi/index.jsp>
- [4] Barnsley, M. J., Strahler, A. H., Morris, K. P., and Muller, J. P., Sampling the surface bidirectional reflectance distribution function (BRDF): 1. Evaluation of current and future satellite sensors, *Remote Sensing Reviews*, vol. 8, pp. 271-311, 1994
- [5] Pinty, B. and Verstraete M., 1992. On the design and validation of surface bidirectional reflectance and albedo model, *Remote Sensing of Environment*, vol. 41, pp. 155-167
- [6] Liang, S., 2003. A direct algorithm for estimating land surface broadband albedos from MODIS imagery, *IEEE Transaction on Geoscience and Remote Sensing*, vol. 41, pp. 136-145
- [7] Asner, G. P., Braswell, B. H., Schimel, D. S., and Wessman, C. A., Ecological research needs from multiangle remote sensing data, *Remote Sensing of Environment*, vol. 63, pp. 155-165, 1998
- [8] Liang, S., 2000. Narrowband to broadband conversions of land surface albedo I - Algorithms, *Remote Sensing of Environment*, vol. 76, pp. 213-238
- [9] Liang, S., Shuey, C. J., Russ, A. L., Fang, H., Chen M., Walthall C. L., Daughtry, C. S. T. and Hunt, R., 2002. Narrowband to broadband conversions of land surface albedo: II. Validation, *Remote Sensing of Environment*, vol. 84, pp. 25-41
- [10] Chander, G. and Markham, B., 2003. Revised Landsat-5 TM Radiometric Calibration Procedures and Postcalibration Dynamic Ranges, *IEEE Transactions on Geoscience and Remote Sensing*, Vol. 41, No. 11, pp. 2674-2677
- [11] Weng, Qihao., Lu, D. and Schubring, J., 2004. Estimation of land surface temperature-vegetation abundance relationship for urban heat island studies, *Remote Sensing of Environment*, vol. 89, pp. 467-483
- [12] Li, F. Jackson, T. J., Kustas, W. P., Schmugge, J., French, A. N., Cosh, M. H. and Bindlish, R., 2004 Deriving land surface temperature from Landsat 5 and 7 during SMEX02/SMACEX, *Remote Sensing of Environment*, vol. 92, pp. 521-534
- [13] Sobrino, J. A., Raissouni, N., and Li, Z., 2001. A comparative study of land surface emissivity retrieval from NOAA data, *Remote Sensing of Environment*, vol. 75, pp. 256-266
- [14] Choudhury, B. J., Ahmed, N. U., Idso, S. B., Reginato, R. J., and Daughtry, C. S. T., 1994. Relations between evaporation coefficients and vegetation indices studied by model simulation, *Remote Sensing of Environment*, vol. 50 pp. 1-17
- [15] eCognition, available at <http://www.definiens-imaging.com/>
- [16] Landsat 7 Science Data Users Handbook, available at http://ltpwww.gsfc.nasa.gov/IAS/handbook/handbook_htmls/chapter11/chapter11.html

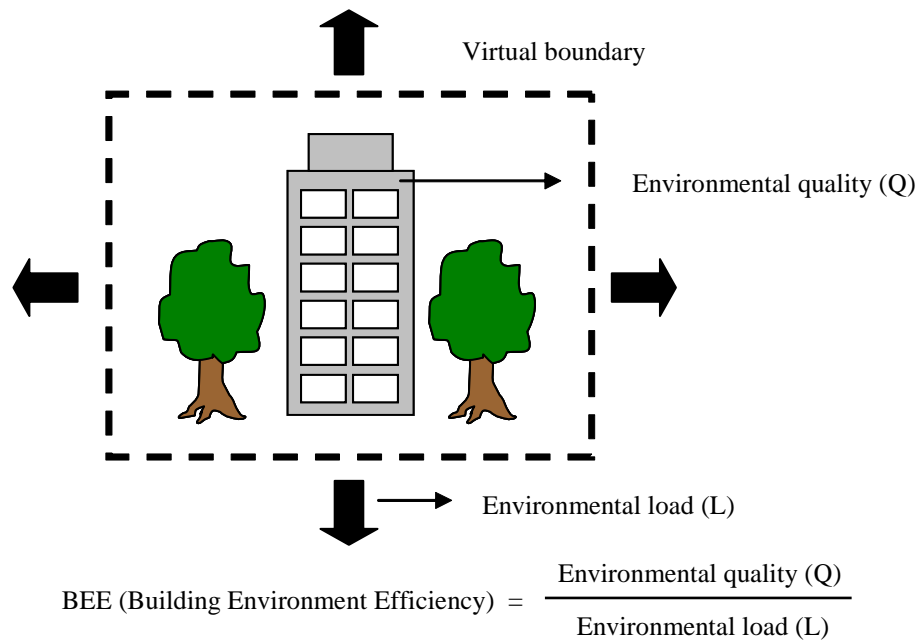


Figure 1: Basic concept of CASBEE. BEE (Building Environment Efficiency) can be defined as the ratio of “Environmental quality” to “Environmental load” [2].

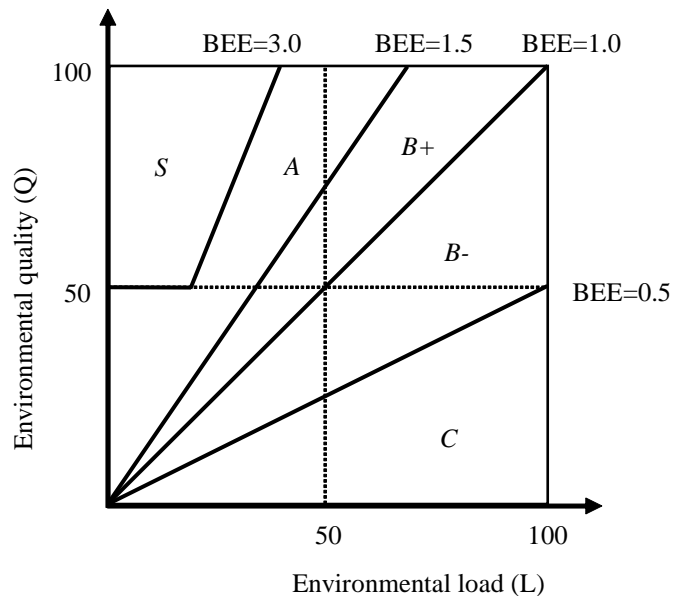


Figure 2: Example of assessment of environmental quality and load based on BEE. BEE value enables the comparison between different buildings. This framework of CASBEE can be applied for environmental indices for urban sustainability, or EIUS [2].

Table 1: Framework of EUIS and results of data collection in Bangkok. Gray column represents data were not available in Bangkok.

Quality of Life Inside City				
First Classification	Second Classification	Third Classification	Source	
Environment/ Public Health	Degree of nature	Ratio of vegetation coverage		
	Sanitary conditions <input type="checkbox"/> <input type="checkbox"/>	Cases of grievances against pollution		PCD
		Distribution ratio of sewerage (%)		BMA
		Air pollution concentration along main roads		PCD
		Cases of oxidase smog		---
		Ratio of patients of breathing diseases		MPH/BMA(DMS)
		Ratio of patients of infectious diseases		MPH/BMA(DMS)
		SO ₂ Density (ppm)		PCD
		NO _x Density (ppm)		PCD
		SPM Density (mg/m ³)		PCD
Public Function/ Public Services	Administration	Growth rate of population (%)	NSO	
		Financial capability index	NSO	
	Habitation	Floor space of houses (□ /one person)		---
		Ratio of electrified areas		
		Ratio of persons equipped with information devices		
	Education	Ratio of graduates studying in elementary schools		BMA/NSO
		the number of teacher at primary school (the number/1,000persons)		BMA/NSO
		the number of the library volumes (the number/one persons)		BMA/NSO
		the number of Infant school (the number/1,000persons)		BMA/NSO
	Commerce	Retail stores(the number/1,000persons)		
	Traffic	Length of roads/Passing transport		PWD
		Modal share of public transport(%)		OTP
	Welfare	Areas of urban parks(□ /person)		BMA
		Medical welfare facilities (the number/one person)		DLP/SSO
Safty/ Security	Earthquake	Ratio of non-earthquake-proof houses (%)	---	
		Fire	Fire occurrences (the number/1,000persons/one year)	BMA (DPS)
		Ratio of non-fire-proof houses (%)		---
		Rescue operation persons of fire station (the number/1000persons)		
	Storm and flood damage	the number of disasters /the volume of rainfalls (the ratio/one year)		DDPM
	Crime/Accident	Criminal offenses (the number/1000persons/one year)		Royal Thai Police
		Traffic accidents (the number/one person/one year)		Royal Thai Police
		Field policemen (the number/1,000persons)		Royal Thai Police
		Beds of sickness (the number/1,000persons)		MPH/BMA(DMS)

Environmental Load				
First Classification	Second Classification	Third Classification	Source	
Energy	Electricity	Consumption of electricity (kWh/one person/one year)	MEA	
	Gas	Consumption of city gas (MJ/one person/one year)	---	
		Consumption of propane gas (kg/one person/one year)		PTT/PTIT
		Consumption of kerosene (ℓ/one person/one year)		EPPO
Resources	Water Resources	Water use (m ³ /one person/one year)	MWA	
	Waste	Household refuse (kg/one person/one year)	BMA	
		Industrial wastes (ton/one person/one year)		DIW
Environment □ over wide area	Atmosphere	CO ₂ Emission Volume (ton/one person/one year)	DAEDE	
		SO ₂ Emission Volume (ton/one person/one year)	DAEDE	
		NO _x Emission Volume (ton/one person/one year)	DAEDE	
		SPM Emission Volume (ton/one person/one year)	DAEDE	

Remarks;

BMA: Bangkok Metropolitan Administration

DAEDE: Department of Alternative Energy Development and Efficiency

DDPM: Department of Disaster Prevention and Mitigation

DDS: Department of Drainage and Sewerage

DEQP: Department of Environmental Quality Promotion

DIW: Department of Industrial Works

DLP: Department of Labour Protection and Welfare

DMS: Department of Medical Services

DPS: Disaster Prevention Subdivision

DPT: Department of Public Works, Town and Country Planning

EPPO: Energy Policy and Planning Office

MEA: Metropolitan Electricity Authority

MPH: Ministry of Public Health

MWA: Metropolitan Waterworks Authority

NSO: National Statistical Office

OTP: Office of Transport and Traffic Policy and Planning

PCD: Pollution Control Department

PTIT: Petroleum Institute of Thailand

PTT: PTT Public Company Limited

PWD: Public Works Department

SSO: Social Security Office

Table 2: Landsat-5 TM and Landsat-7 ETM+ postcalibration dynamic ranges. Units of Lmin and Lmax are $W/(m^2 \cdot sr \cdot \mu m)$ [10] [16]

Band	Landsat 5 TM (from March 1, 1984 to May 4, 2003)		Landsat 7 ETM+ (from July 1, 2000)		
	Lmin	Lmax	Low/High	Low gain	High gain
1	-1.52	152.10	Lmin	Lmax	Lmax
1	-1.52	152.10	-6.2	293.7	191.6
2	-2.84	296.81	-6.4	300.9	196.5
3	-1.17	204.30	-5.0	234.4	152.9
4	-1.51	206.20	-5.1	241.1	157.4
5	-0.37	27.19	-1.0	47.57	31.06
6	1.2378	15.303	0.0	17.04	12.65
7	-0.15	14.38	-0.35	16.54	10.80
8	---	---	-4.7	243.1	158.3

Table 3: TM solar exoatmospheric spectral irradiances. Units is $W/(m^2 \cdot \mu m)$ [10] [16]

Band	Landsat 5 TM	Landsat 7 ETM+
1	1957.000	1970.000
2	1826.000	1843.000
3	1554.000	1555.000
4	1036.000	1047.000
5	215.000	227.100
7	80.720	80.530
8	---	1368.000

Table 4: TM thermal band calibration constants [10] [16]

Units	$W/(m^2 \cdot sr \cdot \mu m)$	<i>Kelvin</i>
Constant	K_1	K_2
Landsat 5 TM	607.76	1260.56
Landsat 7 ETM+	666.09	1282.71

Table 5: TM images used for the analysis. These images were obtained from Web site [10] [16]

Path/Row	129/50	129/51
TM	1994/Oct/25	1994/Oct/25
ETM+	2000/Nov/02	2002/Jan/08

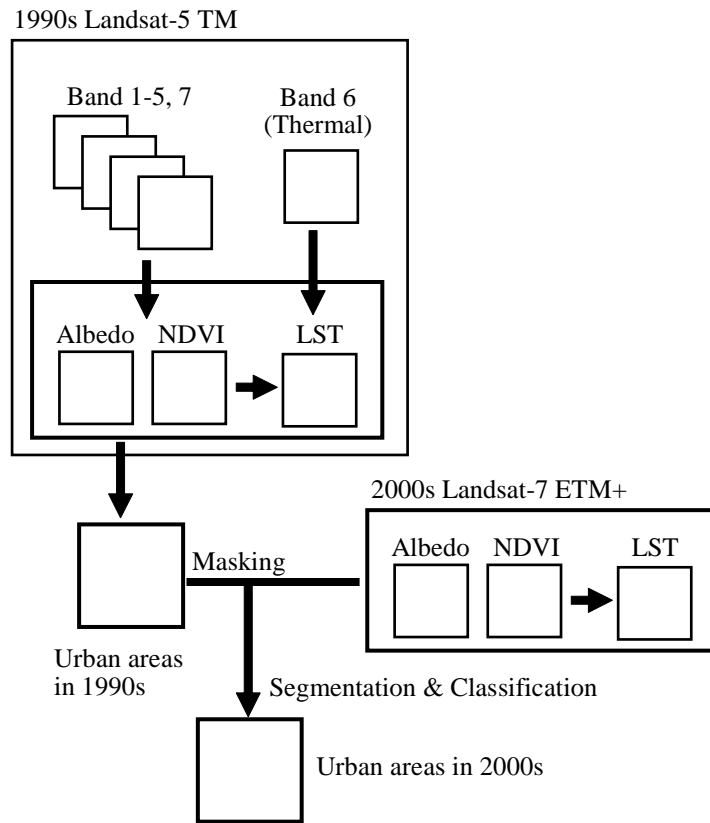


Figure 3: Flow of extraction of urban areas from Landsat TM and ETM+ images

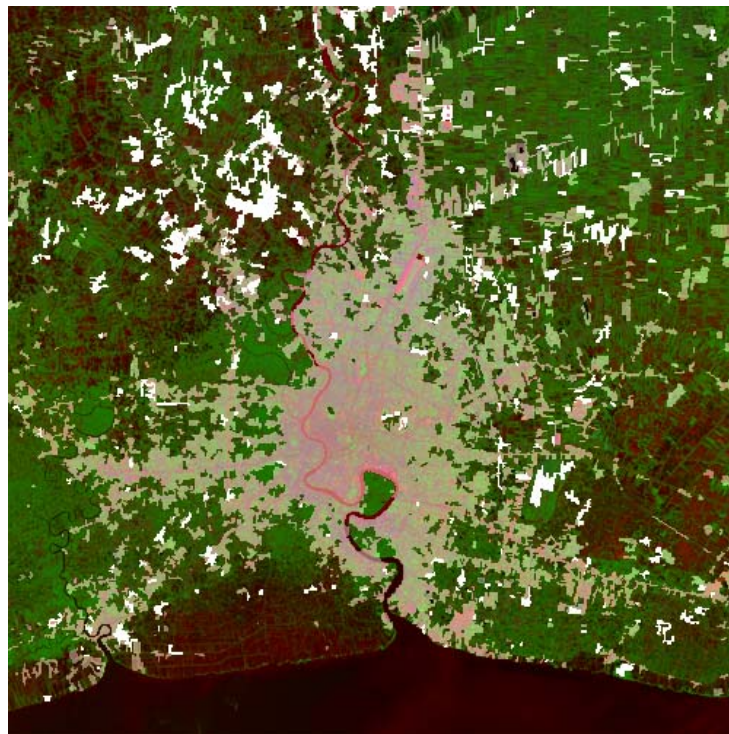


Figure 4: Urban areas of Bangkok, Thailand in 1990s and 2000s extracted from Landsat TM/ETM+ images. A base map is a composite of VIS albedo (red), NDVI (green) and LST (blue) of Landsat ETM+ in 2000s. Gray and white areas represent urban areas since 1990s and urban areas since 2000s, respectively.